administration of Gd-diethylenetriamine pentaacetic acid–*bis* (methylamide: Gd-DPTA–BMA; Omniscan, Daiichi Pharmaceutical Co. Ltd., Tokyo, Japan). There pathologies included Ménière's disease (34 patients), delayed endolymphatic hydrops (8 patients), sudden deafness (5 patients), acute low-tone sensorineural hearing loss (2 patient), fluctuating hearing loss without vertigo (2 patient), bilateral hearing loss without vertigo (1 patient), profound hearing loss with vertigo (1 patient), large vestibular aqueduct syndrome (1 patient), and acoustic tumor (1 patient). In 6 patients (3 with delayed endolymphatic hydrops, 2 with Ménière's disease, and 1 with bilateral profound deafness with vertigo), intratympanic injection was performed in both ears. Thus, 61 ears were included in this study. The diagnosis of each disease was made according to the criteria described in the literature (7–9).

The study protocol was approved by the Ethics Review Committee of Nagoya University School of Medicine (approval nos. 369, 369–2, 369–3, and 369–4). All patients gave their informed consent to participate in this study. The patient's written informed consent was attached to the electronic medical record after he or she gave permission in accordance with the suggestion of the Ethics Review Committee.

Intratympanic Gd Injection

The detailed methods for intratympanic Gd injection have been reported previously (6). Based on the results from this previous study, the scan delay after intratympanic Gd injection was determined as 24 hours to allow the Gd to be distributed widely in the perilymphatic space of the labyrinth.

Gd-DPTA BMA was diluted 8-fold with saline (v/v 1:7) in 58 ears or 16-fold with saline (v/v 1:15) in 3 ears. Because Kakigi et al. (10) reported adverse effects on the stria vascularis when nondiluted Gd was injected into the tympanic cavity of guinea pigs, we tried to use Gd diluted 16-fold to avoid toxicity more securely and compared the results to those obtained with Gd diluted 8-fold.

The patient was placed in the supine position with his or her head turned about 30 degrees away from the sagittal line toward the other ear. The diluted Gd-DPTA BMA was injected intratympanically through the tympanic membrane using a 23-G needle and a 1-ml syringe. In many patients, small gauze soaked by 4% lidocaine was put for 10 minutes before the injection, but in some patients, the injection was done without anesthesia. The amount of diluted Gd injected was 0.4 to 0.5 ml. After the injection, the patient remained in the supine position for 60 minutes with the head turned about 60 degrees away from the sagittal line toward the other ear.

Magnetic Resonance Imaging

Magnetic resonance imaging (MRI) was performed with a 3-Tesla unit in 54 patients (Trio, Siemens, Erlangen, Germany) and a 1.5-Tesla unit in 1 patient because of mechanical problem on the 3-Tesla unit using a receive-only 12-channel phased-array coli. T1-Weighted 3-dimensional fast low-angle shot (3D-FLASH) and conventional 3-dimensional fluid-attenuated inversion recovery (3D-FLAIR) imaging were performed as described previously (11). T2-weighted 3-dimensional constructive interference in the steady-state (3D-CISS) imaging was performed to obtain reference images of labyrinthine fluid-space anatomy.

In 1 patient who underwent the intratympanic Gd injection first, the Gd was not observed in apical turn of cochlea 7 hours later when we undertook twice MRI 1 and 7 hours after the intratympanic Gd injection. MRI performed 1 day after the intratympanic injection of Gd showed that the border of the perilymph and endolymph was clearly visible, and that the Gd was observed almost entirely inside the inner ear. Then we concluded that MRI undertaken 1 day after the intratympanic Gd injection would provide maximum information (12).

RESULTS

Enhancement by 16-fold dilution of Gd intratympanically was fainter than by 8-fold dilution of Gd, although endolymphatic space could be evaluated with the 16-fold dilution of Gd. So, we used eightfold dilution of Gd in the other patients. In 53 ears, the Gd-containing perilymphatic space of the inner ear appeared clearly in the MRI as a high signal on 3D-FLAIR. However, in 2 ears with Ménière's disease and 1 ear with profound deafness with vertigo, movement of Gd into the inner ear was not visible. Figure 1 shows an example of MRI of the inner ear in which the Gd appeared in the perilymphatic space clearly. Figure 2 shows that the movement of Gd into the inner ear was not visible. Of the 3 ears that did not show evidence of movement of Gd into the inner ear, 2 ears had calcification of the tympanic membrane in association with a previous history of otitis media, but 1 ear had no abnormal findings of the tympanic membrane and no history of otitis media. To rule out the possibility of an incorrect method of injection, we repeated the intratympanic injection of Gd into the same ear and MRI, and found the same result (i.e., no evidence of Gd movement into the inner ear).

In 5 ears (4 with Ménière's disease and 1 with delayed endolymphatic hydrops), movement of Gd into the inner ear was observed more faintly than usual (Fig. 3). These 5 ears received the 8-fold dilution of Gd intratympanically, and the Gd density in the inner ear was less than that in the 3 ears treated with the 16-fold dilution of Gd. One of the 5 ears had calcification of the tympanic

FIG. 1. Axial magnetic resonance image. The right inner ear of a 33-year-old man with Ménière's disease. Three-dimensional fluid-attenuated invention recovery magnetic resonance image taken 1 day after intratympanic injection of Gd shows that the Gd is in the basal and second turns of the cochlea, vestibule, and semicircular canals. The *long arrow* indicates the horizontal semicircular canal, and the *short arrow* indicates the posterior semicircular canal.

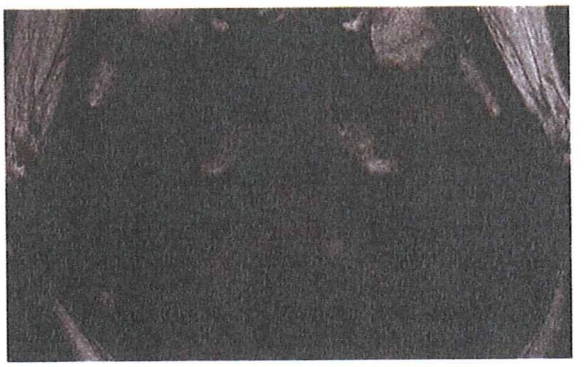

FIG. 2. Axial magnetic resonance image of the right inner ear of a 39-year-old woman with Ménière's disease. Three-dimensional fluid-attenuated invention recovery magnetic resonance image taken 1 day after intratympanic injection of Gd. The high signals of the cochlea are not visible. We injected Gd intratympanically into the same ear again, but the MRI showed no movement of Gd into the inner ear.

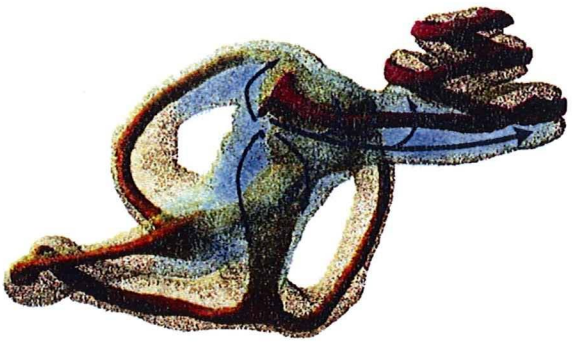

FIG. 4. Schema of Gd distribution inside the perilymph 2 hours after intratympanic Gd injection from an example of the inner ear in which the Gd appeared in the perilymphatic space clearly. The Gd distribution in the perilymph is shown in *light blue*, and the direction of Gd movement is shown in *dark blue*. Two hours after the intratympanic injection, Gd appears in the scala vestibule through the lateral route of the cochlea (*curved arrows*) and not through the helicotrema.

membrane, and 1 ear had slight inflammation in mastoid cells caused by otitis media, which had been diagnosed with computerized tomography (CT); however, 3 of the 5 ears showed no abnormal finding of the tympanic membrane.

DISCUSSION

Figure 4 shows the Gd distribution in the perilymph after 2 hours from the intratympanic injection. The intratympanically administered Gd entered the scala tympani of the cochlea through the round window membrane and moved quickly into the perilymph of the vestibule. On MRIs taken 2 hours after the injection, the Gd was observed in the vestibule, parts of the lateral semicircular canals close to the vestibule, and the scala tympani of the basal turn of the cochlea (6). One day after the intratympanic injection, the Gd had infiltrated a wider area in the semicircular canals and the cochlea, and was observed almost entirely inside the perilymph of the inner ear. Gd appeared in the scala vestibule of the basal turn by way of the lateral wall of the cochlea and not by way of the helicotrema (Fig. 4). These results show that before Gd moves inside the inner ear, it enters through the round window membrane.

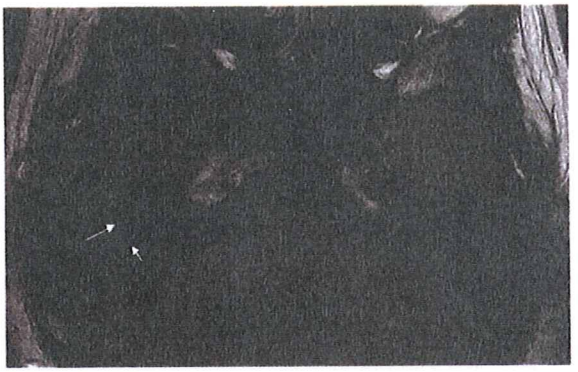

FIG. 3. Axial magnetic resonance image. Right inner ear of a 38-year-old woman with Ménière's disease. Three-dimensional fluid-attenuated invention recovery magnetic resonance image taken 1 day after intratympanic injection of Gd. The *long arrow* indicates the horizontal semicircular canal, and the *short arrow* indicates the posterior semicircular canal. The bright signals of the semicircular canal and the high signals of the cochlea are fainter than usual.

In our experience, Gd did not reach the apical turn of the cochlea when 7 hours passed after the intratympanic injection. Zou et al. (13) reported that Gd was observed in all locations of the inner ear when 12 hours passed after intratympanic Gd injection. Twelve hours of waiting time may be sufficient, but we waited for 24 hours to keep daily works.

We found that the passage of the drug through the round window membrane is poor in 13% of ears even if no active otitis media was present at the time of the intratympanic injection. When considering intratympanic gentamicin therapy in patients with Ménière's disease or intratympanic steroid therapy in patients with sudden sensorineural hearing loss, the clinician should also consider using intratympanically administered Gd to evaluate the permeability of the round window membrane. The results of the intratympanically administered Gd should contribute valuable information for choosing the appropriate treatment.

For 5% of ears that round window permeability was absent by imaging after intratympanic Gd injection, intratympanic drug therapy is not appropriate for the treatment of inner ear diseases. In these patients, we need to choose the treatment excepting intratympanic drug therapy. For 8% of ears that movement of Gd into the inner ear was observed more faintly than usual, we tell the results to patients and talk about treatment plan.

Because Gd entered the inner ear partially, it is possible to choose intratympanic drug therapy. However, the effect may not be sufficient.

Because 87% of patients are likely to have patent and permeable round window membranes, intratympanic drug therapy can be done without the inner ear imaging. Intratympanic Gd injection may be reserved for those not responding to the treatment. When there is no permeability of the round window, intratympanic drug therapy should be abandoned. When the permeability of the round window is not sufficient, treatment plan should be talked with the patients.

The molecular weight of Gd-DPTA BMA is 645.7. Gentamicin is given as one of 3 drugs—gentamicin C1, gentamicin C2, and gentamicin C1a—whose molecular weights are 477.6, 449.5, and 463.6, respectively. Previous researchers have used dexamethasone (392.5) or methylprednisolone (374.5) as intratympanically administrated steroids (14,15). It is thought that the lower the molecular weight, the greater the permeability of the round window membrane (16). However, the Gd movement demonstrated by MRI may be an indicator of movement of intratympanically applied steroids or gentamicin.

CONCLUSION

In patients who are unresponsive to intratympanic gentamicin therapy for the treatment of intractable Ménière's disease, it is probable that the permeability of the round window is impaired. Inner ear MRI after intratympanic Gd administration can be used to assess the permeability of the round window membrane in addition to its use in the evaluation of the endolymphatic space size.

REFERENCES

1. Durland WF Jr, Pyle GM, Connor NP. Endolymphatic sac decompression as a treatment for Ménière's disease. *Laryngoscope* 2005; 115:1454–7.
2. Cohen-Kerem R, Kisilevsky V, Einarson TR, et al. Intratympanic gentamicin for Ménière's disease: a meta-analysis. *Laryngoscope* 2004;114:2085–91.
3. Slattery WH, Fisher LM, Iqbal Z, et al. Intratympanic steroid injection for treatment of idiopathic sudden hearing loss. *Otolaryngol Head Neck Surg* 2005;133:251–9.
4. Allens MJ, der Gaag MA, Stokroos RJ. Intratympanic steroid therapy for inner ear diseases, a review of the literature. *Eur Arch Otorhionolaryngol* 2006;263:792–7.
5. Silverstein H, Rowan PT, Olds MJ, et al. Inner ear perfusion and the role of round window patency. *Am J Otol* 1997;18:586–9.
6. Nakashima T, Naganawa S, Sugiura M, et al. Visualization of endolymphatic hydrops in patients with Meniere's disease. *Laryngoscope* 2007;1173:415–20.
7. Committee on Hearing and Equilibrium. Committee on hearing and equilibrium guidelines for the diagnosis and evaluation of therapy in Meniere's disease. *Otolaryngol Head Neck Surg* 1995; 113:181–5.
8. Nomura Y. Diagnosis criteria for sudden deafness, mumps deafness and perilymphatic fistula. *Acta Otolaryngol Suppl* 1988; 456:7–8.
9. Abe T, Tsuiki T, Murai M, et al. Review of the evaluation criteria for low tone sudden deafness [in Japanese]. *Nippon Jibiinkoka Gakkai Kaiho* 1992;95:7–14.
10. Kakigi A, Nishimura M, Takeda T, et al. Effect of gadolinium injection into the middle ear on the stria vascularis. *Acta Otolaryngol* 2008;128:841–5.
11. Naganawa S, Satake H, Kawamura M, et al. Separate visualization of endolymphatic space, perilymphatic space and bone by a single pulse sequence; 3D-inversion recovery imaging utilizing real reconstruction after intratympanic Gd-DTPA administration at 3 Tesla. *Eur Radiol* 2008;5:920–4.
12. Naganawa S, Sugiura M, Kawamura M, et al. Imaging of endolymphatic and perilymphatic fluid at 3T after intratympanic administration of gadolinium-diethylene-triamine pentaacetic acid. *AJNR Am J Neuroradiol* 2008;29:724–6.
13. Ahn JH, Yoo MH, Yoon TH, et al. Can intratympanic dexamethasone added to systematic steroids improve hearing outcome in patient with sudden deafness? *Laryngoscope* 2008;118:279–82.
14. Zou J, Pyykkö I, Bjelke B, et al. Communication between the perilymphatic scalae and spiral ligament visualized by in vivo MRI. *Audiol Neurotol* 2005;10:145–52.
15. Fitzgerald DC, McGuire JF. Intratympanic steroids for idiopathic sudden hearing loss. *Ann Otol Rhinol Laryngol* 2007; 116:253–6.
16. Juhn SK, HAmaguchi Y, Goycoolea M. Review of round window membrane permeability. *Acta Otolaryngol Suppl* 1989;457:43–8.

Acta Oto-Laryngologica, 2009; 129: 127–131

informa
healthcare

ORIGINAL ARTICLE

Cochlear blood flow during occlusion and reperfusion of the anterior inferior cerebellar artery – effect of topical application of dexamethasone to the round window

HIRONAO OTAKE, HIROSHI YAMAMOTO, MASAAKI TERANISHI, MICHIHIKO SONE & TSUTOMU NAKASHIMA

Department of Otorhinolaryngology, Nagoya University School of Medicine, Nagoya, Japan

Abstract

Conclusion. Topical application of dexamethasone may support autoregulation of cochlear blood flow (CBF), although it had no direct effect on CBF. *Objectives.* Although intratympanic steroid therapy for patients with inner ear disorders is common, the mechanism by which steroids exert their effect is unclear. We investigated the response of CBF to topical application of dexamethasone onto the round window. *Materials and methods.* Two concentrations of dexamethasone (3.3 mg/ml and 33 mg/ml dexamethasone in 0.5 μl saline) were applied to the round windows of rats, and CBF responses were measured using a laser Doppler flowmeter. The effects on CBF of a 2 h occlusion of the anterior inferior cerebellar artery (AICA) and subsequent release of the clamp with or without previous dexamethasone application were investigated. *Results.* No significant change in CBF was observed after topical application of dexamethasone, and it did not affect the decrease in CBF caused by AICA occlusion. However, recovery of CBF after release of the AICA clamp was better in animals treated with dexamethasone than in those that did not receive dexamethasone.

Keywords: *Cochlear blood flow, occlusion, reperfusion, anterior inferior cerebellar artery, dexamethasone*

Introduction

The concentration of steroids in the fluid of the inner ear is significantly greater after local administration of steroids to the round window than after systemic steroid administration [1,2]. Many reports have recently been published on intratympanic steroid therapy for the treatment of sudden deafness. Most of these reports indicate that intratympanic steroid therapy is useful for this purpose [3,4]. Intratympanic steroid therapy has also been used to treat Meniere's disease [5]. Some patients with Meniere's disease benefit from intratympanic steroid therapy, but there is controversy about its efficacy.

Although glucocorticoids are often administered to patients with sudden sensorineural hearing loss, the mechanism by which steroids exert their effects is unclear. Fukushima et al. [6] reported that intratympanic injection of steroids up-regulated aquaporin 1 mRNA in the rat cochlea in a dose-dependent manner. Their results suggest that steroids may affect water homeostasis in the rat inner ear via aquaporin 1. An anti-inflammatory effect of intratympanic steroids on experimentally induced inner ear inflammation has also been described [7].

The effect of local application of steroids to the round window on cochlear blood flow (CBF) has also been investigated. Shirwany et al. [8] observed an initial increase in CBF, which persisted for at least 1 h after intratympanic dexamethasone administration to guinea pigs. Sone et al. [7] investigated the effect of prostaglandin E1 application to the round window on CBF in rats with inner ear inflammation induced by lipopolysaccharide treatment. The elevation in CBF caused by topical application of prostaglandin E1 was greater when dexamethasone was applied intratympanically in advance than when animals received saline instead of dexamethasone. Therefore, CBF may be affected by topical administration of steroids. However, there are no reports of

Correspondence: Tsutomu Nakashima, Department of Otorhinolaryngology, Nagoya University School of Medicine, 65, Tsurumai-cho, Showa-ku, Nagoya 466-8550, Japan. E-mail: tsutomun@med.nagoya-u.ac.jp

(Received 19 February 2008; accepted 24 March 2008)

ISSN 0001-6489 print/ISSN 1651-2251 online
DOI: 10.1080/00016480802078119

the effect of intratympanic steroid treatment on cochlear ischemia.

Many studies have been conducted on the effect of steroids on cerebral blood flow when cerebral edema is present [9,10]. The effect of steroids on focal cerebral ischemia after permanent and temporary occlusion of the middle cerebral artery has also been investigated using rats [11]. In the aforementioned study, high-dose methylprednisolone treatment decreased the volume of the infarct after temporary, but not permanent, focal ischemia. This suggests that high doses of methylprednisolone may be clinically useful if reperfusion can be established. Because there are no reports on the effect of steroids on CBF reperfusion, we investigated the effect of dexamethasone administration to the round window on CBF under normal, ischemic, and reperfusion conditions using laser Doppler (LD) flowmetry.

Materials and methods

Surgical approach

Twenty-five female Sprague Dawley rats (200–280 g, 7–10 weeks old) with normal Preyer's reflexes were used. Experimental protocols were approved by the Nagoya University Committee on the Use and Care of Animals (Permit No. 17082). The rats were anesthetized (i.m.) with 100 mg/kg ketamine and 5 mg/kg xylazine and anesthesia was maintained by supplementary half-doses of ketamine every 60 min. Tracheostomies were performed; all animals breathed spontaneously throughout the experiments. Blood pressure and heart rate were measured using a catheter inserted into the left femoral artery that was connected to a pressure transducer (AS1202, NEC, Tokyo, Japan). Rectal temperature was maintained at 38 ± 1°C using a servoregulated heating blanket.

CBF measurement

The right tympanic bulla was opened using a diamond bur and a ventral–lateral approach. After the middle ear mucosal tissue over the bony wall of the cochlea was gently removed using a cotton pledget, a 1.0 mm diameter LD probe was positioned on the basal turn of the cochlea and connected to an LD flowmeter (ALF21, Advance, Tokyo, Japan) to measure CBF. Petroleum gel was applied to the probe tip to enhance contact between the laser light and the cochlea and to minimize accumulation of blood or fluid underneath the probe. LD and blood pressure data were recorded by a computer every 100 ms.

Administration of dexamethasone

Dexamethasone, a powerful glucocorticoid steroid, was dissolved in saline at concentrations of 3.3 mg/ml or 33 mg/ml. At first, dexamethasone in 0.5 µl saline was administered to the round window and CBF response was observed in five rats at each concentration. Administration of dexamethasone was done after the baseline CBF was confirmed. In 15 rats, the effects on CBF of a 2 h occlusion of the anterior inferior cerebellar artery (AICA) and subsequent release of the clamp with previous dexamethasone or saline application to the round window were investigated. Five rats in group A received saline, five rats in group B received 3.3 mg/ml dexamethasone, and five rats in group C received 33 mg/ml dexamethasone. Among 10 animals in groups A and B, the order of the experiment was random. After that, the experiment in group C rats was performed.

AICA clamping

With the animal's head firmly fixed in a head-holder, the esophagus was transected and muscular attachments to the skull base were excised. A hole was made in the bone at the base of the skull using a diamond burr, and the dura was opened to expose the basilar artery and the AICA. At 30 min after the topical administration to the round window, the right AICA was occluded using the method described previously [12]. A metal rod with a 0.6 mm diameter spherical tip was positioned using a micromanipulator (C1002, Urawa, Tokyo, Japan). Great care was taken not to tear the pia when the metal rod was positioned. The AICA was occluded for 120 min.

Data analysis

Baseline LD output was designated as 100% output. Zero output of the LD flowmeter was designated as 0% output. Data were analyzed using Student's *t* test or analysis of variance (ANOVA) with STATA version 8.0 software. Differences among means were considered statistically significant if the null-hypothesis probability was <0.05. Distributions are expressed as the mean $\pm$ standard deviation (SD).

Results

Topical application of dexamethasone to the round window did not change blood flow volume as estimated from LD flowmeter data. Figure 1 shows blood flow responses to dexamethasone. No significant change in LD output was observed after

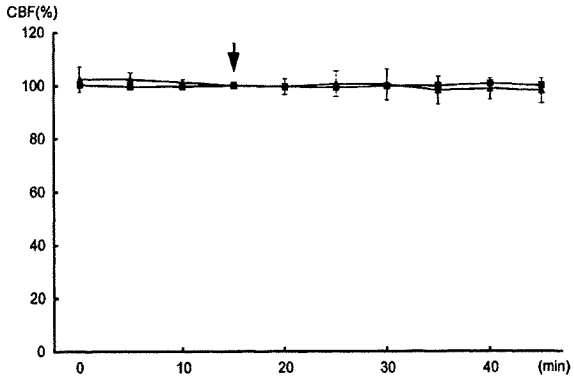

Figure 1. Effect of administration of 0.5 µl dexamethasone to the round window on CBF. The administration was done at the point indicated by the arrow. Squares, 3.3 mg/ml dexamethasone; triangles, 33 mg/ml dexamethasone.

application of either concentration of dexamethasone.

LD output decreased abruptly after AICA clamping, and the low LD output was maintained during the 2 h occlusion of the AICA. When the AICA was occluded after saline administration to the round window (group A; Figure 2), LD values were 50.2 ± 2.7% immediately after occlusion and 47.4 ± 3.0% at 2 h after commencement of the occlusion. After the AICA clamp was released, the LD value increased to 90.9 ± 6.2%. LD values after release of the AICA clamp did not exceed 100% in any of the animals in group A. After the initial elevation upon release of the AICA clamp, the LD value tended to decrease gradually (Figure 2).

For those animals in which the AICA was manipulated after topical administration of 3.3 mg/ml dexamethasone (group B), LD values were 56.4 ± 4.6% immediately after occlusion and 52.5 ± 6.0% at 2 h after commencement of the occlusion. After the AICA clamp was released, the LD value increased to 105.8 ± 8.8% (Figure 3). In four of five animals, the LD value exceeded 100% after release of the clamp. The tendency observed in group A of a decrease in the LD value after the initial abrupt increase consequent to the release of the AICA clamp was not observed in group B.

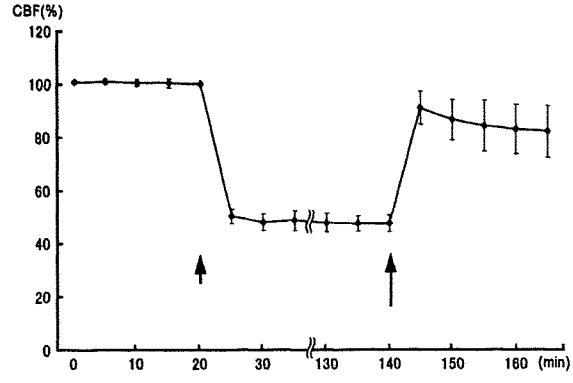

Figure 2. Effect of occlusion and release of AICA on CBF after administration of 0.5 µl saline to the round window. Short arrow indicates beginning of the occlusion, and long arrow indicates the release.

For those animals in which AICA was manipulated after topical administration of 33 mg/ml dexamethasone (group C), LD values were 54.0 ± 8.6% immediately after the occlusion and 52.8 ± 11.7% at 2 h after commencement of the occlusion. After the AICA clamp was released, the LD value increased to 105.0 ± 7.1% (Figure 4). In four of five animals, the LD value exceeded 100% after release of the clamp. The decrease in LD value observed in group A after the abrupt increase caused by the release of the AICA clamp was not observed in group C.

No significant changes in blood pressure were observed after dexamethasone application, AICA clamping or release of the AICA clamp. At the end of the experiment shown in Figures 2–4, mean blood pressure calculated by adding one-third of the pulse pressure to the diastolic pressure was 71.5–49.7 mmHg. The blood pressure did not differ significantly among the three groups.

Among the three groups, blood flow volumes estimated from LD values were compared for each sampling interval after commencement of AICA occlusion. The volumes differed significantly immediately after release of the AICA clamp and for the final measurement (Figures 2–4; $p < 0.05$, ANOVA). There were significant differences between the means of groups A and B for four of the five intervals after release of the AICA clamp and between groups A and C for the first measurement after release of the AICA clamp ($p < 0.05$, t test). However, there were no differences between groups B and C.

Discussion

Tissue hypoxia is intimately associated with inflammatory disease and may constitute a signal for the resolution of inflammatory processes [13–15]. Glucocorticoid signaling, which is mediated through the glucocorticoid receptor, is a clinically important endogenous anti-inflammatory pathway. Microarray analysis has shown that the glucocorticoid receptor is up-regulated by hypoxia [16]. Glucocorticoid receptors are present in the spiral ligament, stria vascularis, organ of Corti, spiral ganglion, and vestibular sensory epithelium of the inner ear. Intratympanically administered dexamethasone rapidly enters the inner ear, where it is converted to its

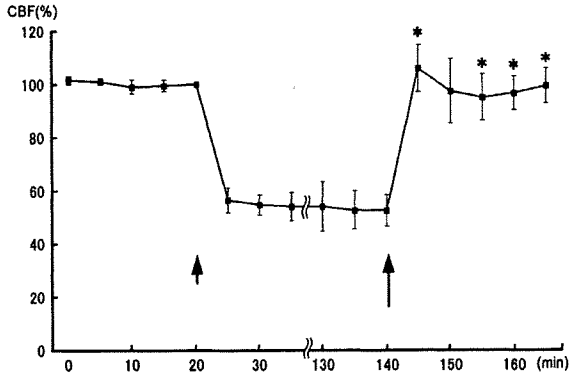

Figure 3. Effect of occlusion and release of AICA on CBF after administration of 0.5 μl dexamethasone (3.3 mg/ml) to the round window. Short arrow indicates beginning of the occlusion, and long arrow indicates the release. Asterisks indicate where there was a significant difference compared with control animals shown in Figure 2.

active form. The distribution of dexamethasone corresponds to that of the glucocorticoid receptor in all tissues of the inner ear except the marginal cells of the stria vascularis [17].

There are few studies on the effects of intratympanic steroid treatment on CBF. Shirwany et al. [8] reported that transtympanic administration of dexamethasone to guinea pigs elevated CBF within 30 s to 29.26%. However, we did not observe any increase in CBF after administration of dexamethasone onto the round windows of rats. Further study is needed to elucidate the response of CBF to topical administration of steroids such as dexamethasone and methylprednisolone, which are now in common use.

After the occlusion of AICA began without leakage of cerebrospinal fluid due to damage to the pia, LD output was stable during the AICA occlusion. During the occlusion, no significant change in the blood flow was observed in each rat, although there were individual differences between animals. The LD probe detects signals from both the cochlea and the bone surrounding the cochlea. The blood supply to the bone originates from the middle ear blood system and differs from the blood supply to the inner ear, which originates from the AICA [18]. LD output during AICA occlusion originates mainly from blood flow in the bone surrounding the cochlea because there is no CBF during AICA occlusion in rats [12]. However, in guinea pigs, CBF tended to recover during AICA occlusion [19]. Therefore, CBF during AICA occlusion differs between rats and guinea pigs.

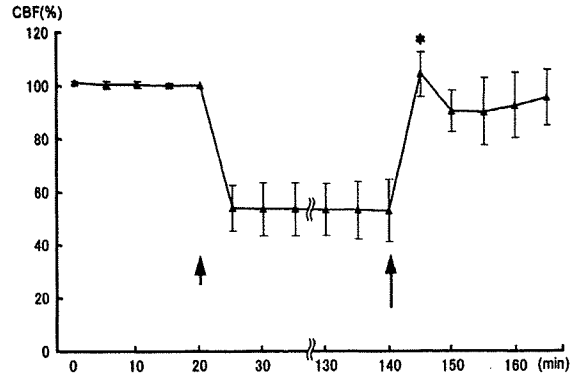

Figure 4. Effect of occlusion and release of AICA on CBF after administration of 0.5 μl dexamethasone (33 mg/ml) to the round window. Short arrow indicates beginning of the occlusion, and long arrow indicates the release. Asterisk indicates where there was a significant difference compared with control animals shown in Figure 2.

After release of the AICA clamp, the autoregulatory rebound phenomenon in which blood flow exceeds 100% of baseline is significant when the occlusion time is relatively short. However, if occlusion is sustained, the rebound phenomenon is minimal or absent. Impaired autoregulation of blood flow may be caused by damage to blood vessels associated with edema. We occluded the AICA for 2 h and found that autoregulation was present when dexamethasone had previously been applied to the round window. The applied dexamethasone may reduce the edema of the inner ear and support autoregulation of CBF. However, additional experiments done with 33 mg/ml dexamethasone did not elevate the autoregulation compared to that done with 3.3 mg/ml. A dexamethasone concentration of 3.3 mg/ml, which is commonly used under clinical conditions, may be sufficient to support autoregulation of CBF after occlusion of the feeder artery.

A protective effect of systemic glucocorticoid administration against ischemia–reperfusion injury of the outer hair cells has been reported for guinea pigs [20]. Attenuation of ischemia-induced damage or reperfusion injury by pretreatment with glucocorticoids has been reported for various organs [16] including the brain. However, glucocorticoids sometimes aggravate ischemia-induced damage [9]. Whether glucocorticoids exert beneficial or adverse effects in ischemia-related injury of the brain may depend on local conditions.

Our study indicates that intratympanic dexamethasone treatment helps maintain autoregulation of CBF after occlusion of the feeder artery. Hearing was not evaluated in this study because intratympanic dexamethasone application affects the middle ear system. However, intratympanic steroid therapy is now widely used for treatment of inner ear diseases. Further histological and functional studies, including hearing tests, on the effects of topical administration of glucocorticoids are warranted.

Declaration of interest: The authors report no conflicts of interest. The authors alone are responsible for the content and writing of the paper.

References

[1] Yang J, Wu H, Zhang P, Hou DM, Chen J, Zhang SG. The pharmacokinetic profiles of dexamethasone and methylprednisolone concentration in perilymph and plasma following systemic and local administration. Acta Otolaryngol 2007;Oct 4:1–9 [Epub ahead of print].

[2] Bird PA, Begg EJ, Zhang M, Keast AT, Murray DP, Balkany TJ. Intratympanic versus intravenous delivery of methylprednisolone to cochlear perilymph. Otol Neurotol 2007;28: 1124–30.

[3] Kilic R, Safak MA, Oguz H, Kargin S, Demirci M, Samim E, et al. Intratympanic methylprednisolone for sudden sensorineural hearing loss. Otol Neurotol 2007;28:312–6.

[4] Ahn JH, Han MW, Kim JH, Chung JW, Yoon TH. Therapeutic effectiveness over time of intratympanic dexamethasone as salvage treatment of sudden deafness. Acta Otolaryngol 2007;Aug 22:1–4 [Epub ahead of print].

[5] Dodson KM, Woodson E, Sismanis A. Intratympanic steroid perfusion for the treatment of Meniere's disease: a retrospective study. Ear Nose Throat J 2004;83:394–8.

[6] Fukushima M, Kitahara T, Uno Y, Fuse Y, Doi K, Kubo T. Effects of intratympanic injection of steroids on changes in rat inner ear aquaporin expression. Acta Otolaryngol 2002; 122:600–6.

[7] Sone M, Hayashi H, Yamamoto H, Tominaga M, Nakashima T. A comparative study of intratympanic steroid and NO synthase inhibitor for treatment of cochlear lateral wall damage due to acute otitis media. Eur J Pharmacol 2003; 482:313–8.

[8] Shirwany NA, Seidman MD, Tang W. Effect of transtympanic injection of steroids on cochlear blood flow, auditory sensitivity, and histology in the guinea pig. Am J Otol 1998; 19:230–5.

[9] Heinonen K, Fedinec A, Leffler CW. Dexamethasone pretreatment attenuates cerebral vasodilative responses to hypercapnia and augments vasoconstrictive responses to hyperventilation in newborn pigs. Pediatr Res 2003;53: 260–5.

[10] Akdemir G, Ergungor MF, Sezer M, Albayrak L, Daglioglu E, Kilinc K. Therapeutic efficacy of intraventricular cyclosporine A and methylprednisolone on a global cerebral ischemia model in rats. Neurol Res 2005;27:827–34.

[11] Slivka AP, Murphy EJ. High-dose methylprednisolone treatment in experimental focal cerebral ischemia. Exp Neurol 2001;167:166–72.

[12] Nakashima T, Suzuki T, Iwagaki T, Hibi T. Effects of anterior inferior cerebellar artery occlusion on cochlear blood flow – a comparison between laser-Doppler and microsphere methods. Hear Res 2001;162:85–90.

[13] Cummins EP, Comerford KM, Scholz C, Bruning U, Taylor CT. Hypoxic regulation of NF-kappaB signaling. Methods Enzymol 2007;435:479–92.

[14] Ruas JL, Lendahl U, Poellinger L. Modulation of vascular gene expression by hypoxia. Curr Opin Lipidol 2007;18: 508–14.

[15] Frede S, Berchner-Pfannschmidt U, Fandrey J. Regulation of hypoxia-inducible factors during inflammation. Methods Enzymol 2007;435:405–19.

[16] Leonard MO, Godson C, Brady HR, Taylor CT. Potentiation of glucocorticoid activity in hypoxia through induction of the glucocorticoid receptor. J Immunol 2005;174:2250–7.

[17] Hargunani CA, Kempton JB, DeGagne JM, Trune DR. Intratympanic injection of dexamethasone: time course of inner ear distribution and conversion to its active form. Otol Neurotol 2006;27:564–9.

[18] Nakashima T, Naganawa S, Sone M, Tominaga M, Hayashi H, Yamamoto H, et al. Disorders of cochlear blood flow. Brain Res Brain Res Rev 2003;43:17–28.

[19] Ren T, Nuttall AL, Miller JM. Contribution of the anterior inferior cerebellar artery to cochlear blood flow in guinea pig: a model-based analysis. Hear Res 1993;71:91–7.

[20] Tabuchi K, Oikawa K, Murashita H, Hoshino T, Tsuji S, Hara A. Protective effects of glucocorticoids on ischemia-reperfusion injury of outer hair cells. Laryngoscope 2006; 116:627–9.

Acta Oto-Laryngologica, 2009; 129: 239–243

informa
healthcare

ORIGINAL ARTICLE

Imaging analysis in cases with inflammation-induced sensorineural hearing loss

MICHIHIKO SONE[1], TERUKAZU MIZUNO[1], SHINJI NAGANAWA[2] & TSUTOMU NAKASHIMA[1]

[1]*Department of Otorhinolaryngology, Nagoya University Graduate School of Medicine, Nagoya, Japan and* [2]*Department of Radiology, Nagoya University Graduate School of Medicine, Nagoya, Japan*

Abstract

Conclusion. 3D-FLAIR imaging is sensitive to inflammatory inner ear disturbances and may be a useful method in investigating the severity of inner ear disturbance in cases of inflammation-induced SNHL. *Objective.* To evaluate the usefulness of the three-dimensional fluid-attenuated inversion recovery (3D-FLAIR) magnetic resonance imaging (MRI) sequence in investigating different etiology of inner ear disturbances in cases with inflammation-induced acute sensorineural hearing loss (SNHL). *Patients and methods.* Five cases with inflammation-induced acute SNHL by different conditions are included in this study: acute meningitis, acute otitis media, and Wegener granulomatosis. Imaging analysis was performed using a three-dimensional fluid-attenuated inversion recovery (3D-FLAIR) magnetic resonance imaging (MRI) sequence, and correlation between clinical symptoms and FLAIR abnormalities was evaluated. *Results.* In the affected ears in all cases, 3D-FLAIR revealed high pre-contrast signal and increased signal in the cochlea after the administration of gadolinium. Enhancement was still observed in the inner ear after several months with continuing nystagmus in those cases induced by meningitis and severe otitis media. In a case with Wegener granulomatosis, increased signal in the post-contrast images was stronger on the side of the cochlea with the worse hearing level.

Keywords: *Inflammation, etiology, sensorineural hearing loss, inner ear disturbance, 3D-FLAIR*

Introduction

Inflammatory conditions that occur outside the inner ear, such as otitis media or meningitis, can induce inner ear disturbances with symptoms of sensorineural hearing loss (SNHL). Animal studies have investigated the mechanisms of inflammation-induced inner ear disturbances [1–5]; however, etiological investigations in clinical cases are limited.

Previous reports describe the usefulness of gadolinium enhancements in magnetic resonance imaging (MRI) for detecting inflammatory lesions of the inner ear [6–9]; this enhancement has been considered the result of breakdown of the blood–labyrinth barrier (BLB) [6,8,9]. The BLB maintains the composition of the inner ear fluid; its function is to protect the inner ear from toxic substances by selectively limiting the entry of substances into the inner ear [10]. The fluid-attenuated inversion recovery (FLAIR) MRI sequence has been recently applied to the inner ear [11–13]. FLAIR enables the demonstration of hemorrhage and high protein concentration in lesions; these conditions are difficult to detect using T1- and T2-weighted MRI [14]. FLAIR assessment can also be used to evaluate cerebrospinal fluid (CSF) changes in pathologic conditions that cause a breakdown in the blood–brain barrier [15].

In the present paper, we apply 3D-FLAIR MRI at three tesla to cases with inflammation-induced acute SNHL caused by different conditions, and evaluate the results with the aim of demonstrating its advantage in investigating etiologies in these inner ear disturbances.

Materials and methods

Patients

Five cases with inflammation-induced acute SNHL and by different conditions were included in this

Correspondence: Michihiko Sone, Department of Otorhinolaryngology, Nagoya University Graduate School of Medicine, 65 Tsurumai-cho, Showa-ku Nagoya 466–8550, Japan. Tel: +81 52 744 2323. Fax: +81 52 744 2325. E-mail: michsone@med.nagoya-u.ac.jp

(Received 15 April 2008; accepted 22 May 2008)

ISSN 0001-6489 print/ISSN 1651-2551 online
DOI: 10.1080/00016480802226163

study: acute meningitis (1 case), acute otitis media (2 cases), and Wegener granulomatosis in the middle ear (2 cases).

MRI examination

MRI was performed using a three-tesla scanner (Trio, Siemens, Erlangen, Germany). 3D-FLAIR was performed before and after the intravenous administration of a single dose of gadolinium. To delineate the anatomy of the CSF space, we performed heavily T2-weighted 3D constructive interference imaging in the steady state prior to the administration of contrast material. High signal on 3D-FLAIR after contrast enhancement was scored depending by the degree of the enhancement as follows: weak = 1, moderate = 2, and strong = 3.

Results

The clinical observation and the MRI findings in the five cases are summarized in Tables I and II. 3D-FLAIR images in five cases showed high pre-contrast signal in the cochlea, the vestibule, and the semicircular canals in the inner ear, while the post-contrast images demonstrated enhancement in the inner ear of the affected ears. High post-contrast signals examined after treatment were decreased in all cases except one (Case 2), which were accompanied by improvement in symptoms of vertigo (Cases 1 and 4), and acute SNHL (Cases 3, 4, and 5). The post-contrast images were not available in one patient because of complete ossification of the cochlea (Case 1). Correlation between clinical symptoms and FLAIR abnormalities was observed in some cases. Representative cases from different condition were described below.

Acute meningitis (Case 1)

A 42-year-old man was hospitalized because of impaired consciousness, the cause of which was diagnosed as acute meningitis. He had had severe vertigo and profound SNHL on the left side. Six months later the patient again suffered acute meningitis and was referred to our department to investigate the possibility of otitis media-induced meningitis. The patient had chronic otitis media with a perforated tympanic membrane on the left side; however, he had had no experience of ear discharge for years. A computerized tomography (CT) examination demonstrated partial ossification in the cochlea on the left side, which was considered to be due to preceding meningitis. 3D-FLAIR revealed high signal intensity in the cochlea of the inner ear on the left side and strongly increased signal in this area after the administration of gadolinium (Figure 1A,B). Enhancement was also observed in the area of the cochlear aqueduct (Figure 1C) and in the fundus of the internal auditory canal. Otitis media was ruled out as a cause of meningitis in this case; however, during follow-up it was revealed that he had had fine spontaneous nystagmus with fast phase beating contralateral to the affected ear for one year.

Acute otitis media (Case 2)

A 35-year-old man who had been hospitalized at another hospital because of ear discharge and acute SNHL on his left side was referred to our department two months after the onset of the disease. The patient had nystagmus to the right and profound SNHL on the left side, and his disease was diagnosed as severe labyrinthitis caused by acute otitis media. 3D-FLAIR revealed high signal intensity in the cochlea, the vestibule, and the semicircular canals of inner ear on the left side and strongly increased signals in these areas after the administration of gadolinium (Figure 2A, B). This enhancement was also observed one year after onset; at that time he still had fine nystagmus with fast phase beating contralateral to the affected ear.

Wegener granulomatosis (Case 4)

A 69-year-old man was referred to our department with a history of bilateral acute SNHL for three months and facial palsy on his right side for two weeks. The patient's hearing level was worse in the right ear than the left, and he noticed vertigo. The patient had been treated for bilateral otitis media

Table I. Clinical observation in five cases.

	Age (years)/gender	Symptom of inner ear disturbance	Diagnosis (cause)
Case 1	42/M	Vertigo, acute SNHL	Bacterial meningitis
Case 2	35/M	Vertigo, acute SNHL	Acute otitis media
Case 3	79/M	Acute SNHL	Acute otitis media
Case 4	69M	Vertigo, acute SNHL	Wegener granulomatosis
Case 5	45/F	Acute SNHL	Wegener granulomatosis

SNHL, sensorineural hearing loss.

Table II. 3D-flair MRI findings in five cases.

	High signal (at the initial visit)		High signal (post-treatment)
	Pre-contrast	Post-contrast	Post contrast
Case 1	Cochlea, CA	Cochlea (3), fundus (3), CA (3)	NA
Case 2	Cochlea, vestibule, Scc	Cochlea (3), vestibule (2), Scc (1)	Cochlea (3), vestibule (2), Scc (1)
Case 3	Cochlea	Cochlea (1)	None
Case 4	Cochlea, vestibule, Scc	Cochlea (3), vestibule (2), Scc (2)	Cochlea (2)
Case 5	Cochlea, Scc	Cochlea (1), Scc (1)	Cochlea (1)

CA, cochlear aqueduct; Scc, semicircular canal; Fundus, fundus of the internal auditory canal; NA, not available.

with effusion for one year. CT examination revealed widespread inflammation in the bilateral middle ear cavities; however, the inner ear appeared normal. 3D-FLAIR revealed high signal intensity in the cochlea, the vestibule, and the semicircular canals of the inner ear on both sides and increased signal in these areas after the administration of gadolinium, especially in the right ear (Figure 3A, B). Final diagnosis was Wegener granulomatosis, which was treated by chemotherapy with prednisolone and cyclophosphamide. 3D-FLAIR MRI performed after six times of the chemotherapy showed decreased post-contrast signals in the inner ear.

Discussion

3D-FLAIR images in five cases showed high pre-contrast signal in the cochlea, the vestibule, and the semicircular canals of the inner ear, while the post-contrast images demonstrated enhancement in the affected areas. This post-contrast enhancement is considered the result of a breakdown in the BLB [6,8,9,11]. The BLB supports inner ear homeostasis by maintaining constant composition of the inner ear fluid [10]; this inner ear system is concentrated in the cochlear lateral wall. Animal studies have shown breakdown of the BLB in the cochlear lateral wall following acute middle ear inflammation and an associated decrease in lateral blood flow [5,16]. Breakdown of the BLB also occurs in meningogenic suppurative labyrinthitis [17]. The findings of the 3D-FLAIR images in the present study support the explanation that etiologies similar to those in the animal studies might have occurred in the present cases.

The 3D-FLAIR images in Case 1 (acute meningitis) showed strongly increased signal in the cochlear aqueduct on the post-contrast images. This finding supports that of a previous study that the cochlear aqueduct could serve as potential pathway for the spread of infection from the meninges to the inner ear [18]. Contrast enhancement observed in

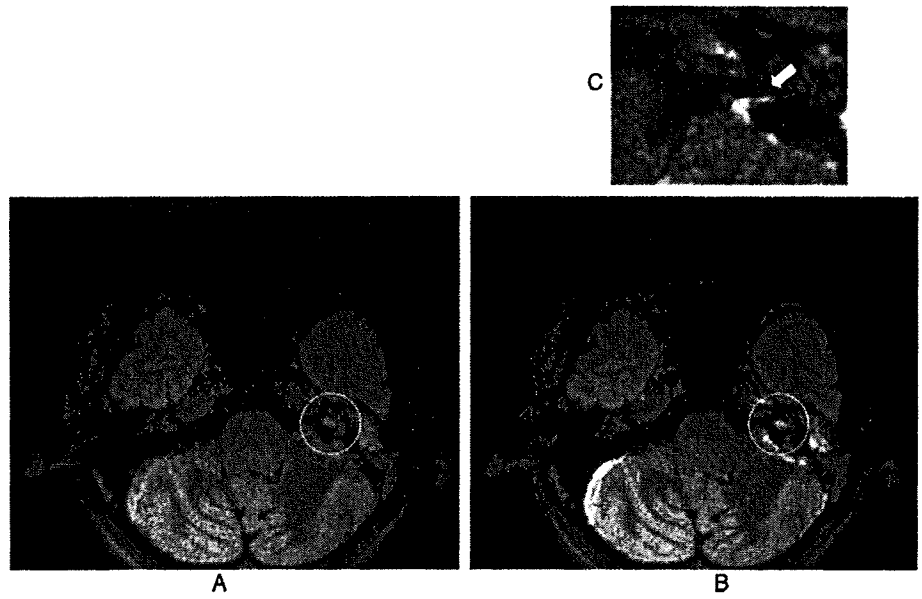

Figure 1. 3D-FLAIR images of Case 1. A, B. Pre-contrast (A) and post-contrast (B) inner ear lesions (circled). The inner ear is morphologically abnormal because of partial ossification. C. High-magnification image of enhancement in the cochlear aqueduct (arrow).

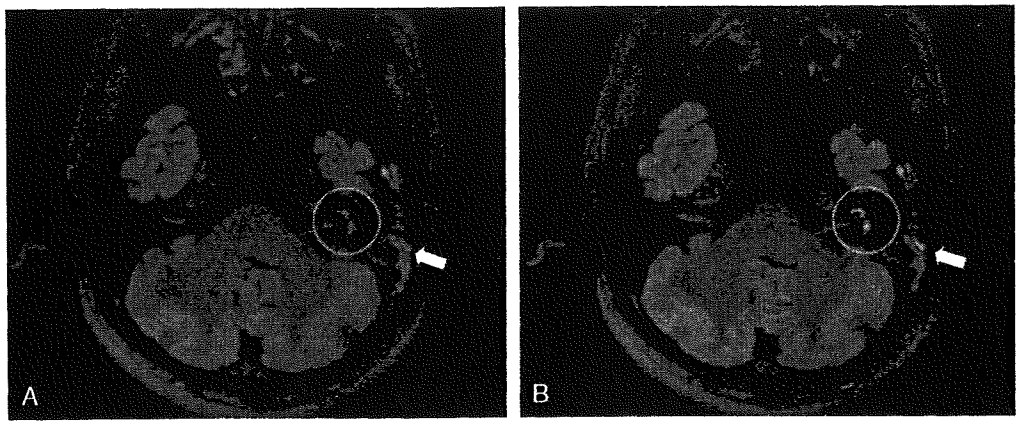

Figure 2. 3D-FLAIR images of Case 2. A, B. Pre-contrast (A) and post-contrast (B) middle ear inflammation (arrows) and inner ear lesions (circled).

the fundus of the internal auditory canal suggests a meningeal rather than otitis media origin as the cause of inner ear disturbance [15].

We have applied 3D-FLAIR to cholesteatoma cases with labyrinthine fistula and usefulness of images of the inner ear has been reported for evaluation of labyrinthine fistula in patients with cholesteatoma [13]. Case 4 with Wegener granulomatosis revealed high signal intensity in the bilateral inner ears. Increased signal of the cochlea in the post-contrast images was stronger on the side with the worse hearing level. SNHL is a significant finding in Wegener granulomatosis, and its detection is important for appropriate patient management [19]. 3D-FLAIR assessment can be a useful method in evaluating the inner ear disturbances caused by Wegener granulomatosis.

Another important finding was the duration over which the high post-contrast signal was observed. Enhancement in inflammatory conditions usually resolves over several months [7]. Decreased signal in the 3D-FLAIR was found in case 3 with mild acute otitis media and cases 4 and 5 with Wegener granulomatosis following treatment with chemotherapy. Hearing improvement was observed in these cases, however, in Cases 1 and 2, in which the

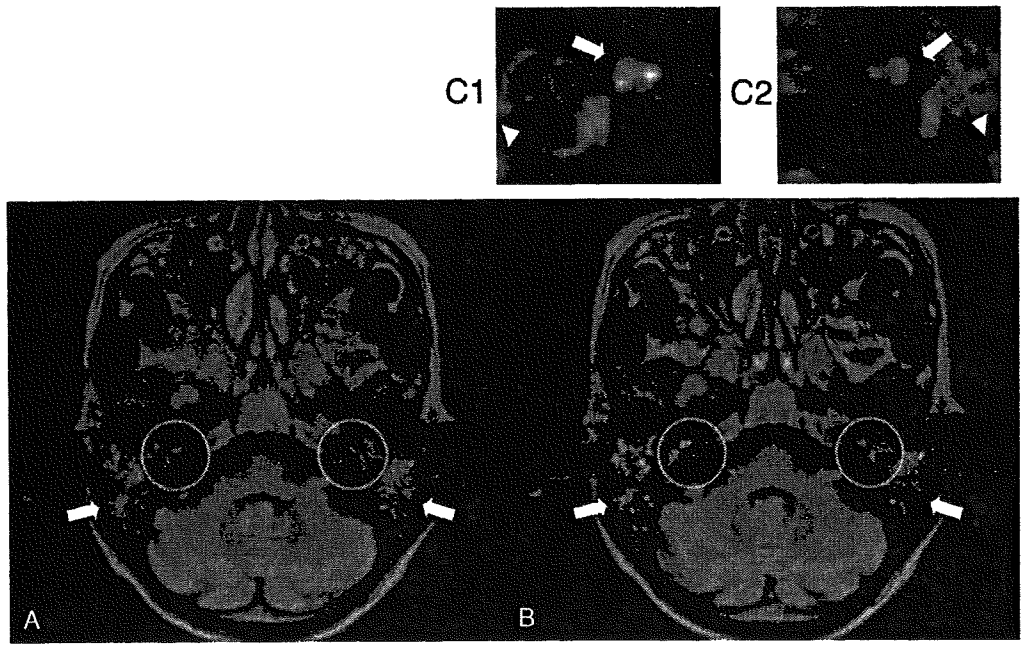

Figure 3. 3D-FLAIR images of Case 4. A, B. Pre-contrast (A) and post-contrast (B) bilateral middle ear inflammation (arrows) and inner ear lesions (circled). A stronger signal is observed in the inner ear on the side with the worse hearing level. C. Higher-magnification image of the lesions circled in B. The cochleas (arrows) and the semicircular canals (arrowheads) are indicated in the right (C1) and left (C2) ears.

patients had continuing nystagmus, high signal was observed in the inner ear over a period of several months. The severity of inner ear disturbances and clinical symptoms may correlate with 3D-FLAIR findings; breakdown of the BLB might last for a longer period in cases with aggressive disease.

Declaration of interest: The authors report no conflicts of interest. The authors alone are responsible for the content and writing of the paper.

References

[1] Morizono T, Giebink GS, Paparella MM, et al. Sensorineural hearing loss in experimental purulent otitis media due to Streptococcus pneumoniae. Arch Otolaryngol 1985; 111:794–8.

[2] Spandow O, Anniko M, Hellstrom S. Inner ear disturbances following inoculation of endotoxin into the middle ear. Acta Otolaryngol 1989;107:90–6.

[3] Watanabe K., Naito N, Tanaka Y. Morphological changes in the inner ear induced by bacterial endotoxin. Med Electron Microsc. 1995;28:80–7.

[4] Sone M., Russlie HQ, Canafax DM, Paparella MM. Expression of intercellular adhesion molecule-1 in rat inner ear due to bacterial otitis media. Ann Otol Rhinol Laryngol. 1999;108:648–52.

[5] Sone M, Hayashi H, Tominaga M, Nakashima T. Changes of cochlear blood flow due to endotoxin-induced otitis media. Ann Otol Rhinol Laryngol 2004;113:450–4.

[6] Mark AS, Seltzer S, Nelson-Drake J, et al. Labyrinthine enhancement on gadolinium-enhanced magnetic resonance imaging in sudden deafness and vertigo: correlation with audiologic and electronystagmographic studies. Ann Otol Rhinol Laryngol 1992;101:459–64.

[7] Mark AS, Fitzgerald D. Segmental enhancement of the cochlea on contrast-enhanced MR: correlation with the frequency of hearing loss and possible sign of perilympatic fistula and autoimmune labyrinthitis. Am J Neuroradiol 1993;14:991–6.

[8] Hegarty JL, Patel S, Fischbein N, Jackler RK, Lalwani AK. The value of enhanced magnetic resonance imaging in the evaluation of endocochlear disease. Laryngoscope 2002;112: 8–17.

[9] Mafee MF. MR imaging of intralabyrinthine schwannoma, labyrinthitis, and other labyrinthine pathology. Otolaryngol Clin North Am 1995;28:407–30.

[10] Juhn SK, Hunter BA, Odland RM. Blood-labyrinth barrier and fluid dynamics of the inner ear. Int Tinnitus J 2001;7: 72–83.

[11] Sugiura M, Naganawa S, Teranishi M, et al. Three-dimentional fluid-attenuated inversion recovery magnetic resonance imaging findings in patients with sudden sensorineural hearing loss. Laryngoscope 2006;116:1451–4.

[12] Cadoni G, Cianfoni A, Agostino S, et al. Magnetic resonance imaging findings in sudden sensorineural hearing loss. J Otolaryngol 2006;35:310–6.

[13] Sone M, Mizuno T, Sugiura M, Naganawa S, Nakashima T. Three-dimensional fluid-attenuated inversion recovery magnetic resonance imaging investigation of inner ear disturbances in cases of middle ear cholesteatoma with labyrinthine fistula. Otol Neurotol 2007;28:1029–33.

[14] Naganawa S, Koshikawa T, Nakamura T, et al. Comparison of flow artifacts between 2D-FLAIR and 3D-FLAIR sequences at 3 T. Eur Radiol 2004;14:1901–8.

[15] Bozzao A, Floris R, Fasoli F, et al. Cerebrospinal fluid changes after intravenous injection of gadolinium chelate: Assessment by FLAIR imaging. Eur Radiol 2003;13:592–7.

[16] Sone M, Hayashi H, Yamamoto H, Tominaga M, Nakashima T. A comparative study of intratympanic steroid and NO synthase inhibitor for treatment of cochlear lateral wall damage due to acute otitis media. Eur J Pharmacol 2003; 482:313–8.

[17] Kastenbauer S, Klein M, Koedel U, Pfister HW. Reactive nitrogen species contribute to blood–labyrinth barrier disruption in suppurative labyrinthitis complicating experimental pneumococcal meningitis in the rat. Brain Res 2001;904: 208–17.

[18] Merchant SN, Gopen Q. A human temporal bone study of acute bacterial meningogenic labyrinthitis. Am J Otol 1996; 17:375–85.

[19] Bakthavachalam S, Driver MS, Cox C, et al. Hearing loss in Wegener's granulomatosis. Otol Neurotol 2004;25:833–7.

Eur Arch Otorhinolaryngol (2009) 266:351–355
DOI 10.1007/s00405-008-0745-2

OTOLOGY

Detection of cytomegalovirus DNA in preserved umbilical cords from patients with sensorineural hearing loss

Terukazu Mizuno · Saiko Sugiura · Hiroshi Kimura · Yoshihiro Ando · Michihiko Sone · Yukihiro Nishiyama · Tsutomu Nakashima

Received: 30 December 2007 / Accepted: 2 June 2008 / Published online: 18 June 2008

Abstract We performed a retrospective diagnostic study of congenital cytomegalovirus (CMV) infection in patients with sensorineural hearing loss (SNHL). CMV DNA in preserved umbilical cords was analyzed using real-time polymerase chain reaction analysis. Of 45 analyzable patients with SNHL, CMV DNA was detected in the preserved umbilical cords of 3 patients, all of whom had bilateral SNHL that lacked a clear onset period. CMV DNA was not detected in any of the patients with sudden SNHL or enlarged vestibular aqueduct-associated SNHL. The features of CMV-associated SNHL were more asymmetric than those of CMV-negative bilateral SNHL.

Keywords Cytomegalovirus · Hearing loss · Enlarged vestibular aqueduct · Real-time polymerase chain reaction

T. Mizuno (✉) · S. Sugiura · M. Sone · T. Nakashima
Department of Otorhinolaryngology,
Graduate School of Medicine, Nagoya University,
Nagoya 466-8550, Japan
e-mail: mizuteru@med.nagoya-u.ac.jp

H. Kimura · Y. Nishiyama
Department of Virology, Graduate School of Medicine,
Nagoya University, Nagoya 466-8550, Japan

H. Kimura
Department of Pediatrics, Graduate School of Medicine,
Nagoya University, Nagoya 466-8550, Japan

Y. Ando
Aichi Children's Health and Medical Center,
Obu 474-8710, Aichi, Japan

Introduction

Cytomegalovirus (CMV) infection is the most frequent congenital infection in humans, and congenital CMV infection has been identified as one of the leading causes of sensorineural hearing loss (SNHL) in children [1]. Most infected newborns are asymptomatic, although they are at risk for developing SNHL [2, 3]. Delayed onset SNHL in patients with congenital CMV infection is characterized by fluctuating, progressive, and asymmetric hearing loss [4]. These clinical characteristics are similar to those of enlarged vestibular aqueduct (EVA)-associated SNHL. Studies investigating the relationship between EVA-associated SNHL and congenital CMV infection have been performed [5, 6], but the etiology of sudden SNHL is still not known. Moreover, the relationship between sudden SNHL and congenital CMV infection has not been investigated. Currently, in most asymptomatic infants, the diagnosis of congenital CMV infection is missed during the neonatal period, and the possibility exists that CMV infection is an etiologic factor in some cases of SNHL that lack an obvious cause. However, retrospective diagnosis of congenital CMV infection has been difficult.

Obstetric hospitals in Japan have traditionally provided the dried umbilical cord to every parent as a symbol of the bond between mother and child. These dried cords are stored forever in the home. Recently, the feasibility of using dried umbilical cords for retrospective diagnosis of congenital CMV infection was reported [7–11]. In the present study, we performed a retrospective diagnosis of congenital CMV infection using preserved umbilical cords from patients with various kinds of SNHL to clarify the relationship between SNHL and congenital CMV infection.

Materials and methods

Study population

Fifty patients with SNHL were enrolled in this study. Ten patients had sudden SNHL (group A), seven patients had EVAs (group B), 16 patients had unilateral SNHL without a clear onset period (group C), and 17 patients had bilateral SNHL without a clear onset period (group D). All the patients had uneventful births, and their neonatal courses were unremarkable. Patients with apparent congenital CMV infection-associated SNHL were excluded from the study. The respective age ranges of each group at entry were as follows: Group A, 6–52 years (mean 28.9 years); B, 6–44 years (mean 16.5 years); C, 1–18 years (mean 8.6 years); and D, 2 months to 42 years (mean 12.9 years).

As positive controls, three infants with previously known congenital CMV infections were investigated. At enrollment, their ages were 36, 19, and 20 months. All three infants had bilateral SNHL and impaired motor or intellectual development. An association with CMV was confirmed by serology and typical radiological images of the central nervous system. As negative controls, 10 healthy individuals with normal hearing levels were also examined. They consisted of four male and six female subjects, and their age range was from 1 to 33 years (mean 10.8 years).

Audiometric evaluation

Audiometric evaluation was performed for each patient by pure tone audiometry using the average of 0.5, 1, and 2 kHz. Hearing levels were measured by an experienced audiologist using a clinical audiometer (RION-AA79S; RION Co., Ltd, Tokyo, Japan). When patients were too young to evaluate their hearing ability by pure tone audiometry, auditory brain stem response (ABR) was used. Otoscopic examination and tympanometry were performed before ABR assessment. Children were tested in a quiet room while sleeping. CYN-AX2100 (NEC, Tokyo, Japan) was used to record ABR. The stimuli were clicks at a repetition rate of 9.5/s with 10 dB step increases in intensity. Responses to 1,000 clicks were averaged. The threshold of wave *V* was measured as the hearing level of a patient. If the wave *V* could not be measured by the stimulation of 100 dB nHL, the hearing level was assumed to be 110 dB nHL.

Sample preparation

Preserved umbilical cords were collected from patients and controls. Umbilical cords had been preserved for 2 months to 52 years (mean 16.7 years). For the polymerase chain reaction (PCR) assay, about 5 mg of tissue was cut from the dried cords. DNA was then extracted using a QIAamp DNA Blood Mini Kit (Qiagen GmbH, Hilden, Germany), eluted in 200 μL of distilled water, and stored at −30°C until analysis.

Real-time quantitative PCR assay

Real-time PCR was conducted using a TaqMan PCR kit and Model 7700 sequence detector (Applied Biosystems, Foster City, CA, USA), as described previously [8, 12, 13]. The PCR primers and fluorogenic probe for CMV DNA were from the immediate early gene [14]. A standard curve was constructed using the threshold cycle values obtained from positive control plasmids containing the target sequences. The threshold cycle values from the clinical sample were plotted on the standard curve, and the copy number was calculated automatically [13, 15]. Samples were defined as negative when the threshold value exceeded 50 cycles.

To examine whether analyzable DNA existed in the preserved umbilical cords, human β-actin DNA was concurrently quantified by real-time PCR using the TaqMan β-actin Control Reagent Kit (Applied Biosystems) [16]. When the amount of human β-actin DNA was too small (less than 4,000 copies/μg DNA), the samples were excluded from the study. The number of analyzable cells in each sample was estimated from the amount of human β-actin DNA, and the amount of CMV DNA was adjusted and expressed per 10^6 cells [16].

As controls, Epstein–Barr virus and human herpesvirus 6 DNA were also quantified by the real-time PCR assay. Sequences of primers and probes were as described elsewhere [15, 16].

Statistical analysis

The software package Stat View J 5.0 (Abacus Concepts Inc., Berkeley, CA, USA) was used for data analysis. Student's *t*-test was applied to compare the mean difference of hearing level between right and left ears.

Ethics approval

This study was approved by the local ethics committee and institutional review board of our hospital. Written informed consent was obtained from either the patients or their guardians.

Results

From the 50 umbilical cords of patients with SNHL, no or little β-actin DNA was detected in 5 patients, who were subsequently excluded from further study. Forty-five patients were thus analyzed, consisting of 9 patients from

Group A, six from Group B, 15 from Group C, and 15 from Group D. The clinical characteristics of each group are summarized in Table 1.

CMV DNA was detected in three cords, all of which were from patients in Group D, who had bilateral SNHL without a clear onset period. The serological examinations indicated that the three patients were seropositive for CMV. Details of the clinical characteristics and quantitative CMV DNA data of the three positive patients are shown in Table 2. All the three patients had asymmetric bilateral SNHL and also had neurological findings as listed in Table 2.

We then compared the difference in the hearing level between the right and left ears in the patients with bilateral hearing loss (group D). The mean difference for the patients with CMV-positive bilateral SNHL was 45.7 dB, while those with CMV-negative bilateral SNHL showed a mean difference of 10.8 dB. The difference between the right and left ears was significantly larger in the patients who were CMV-positive than those who were CMV-negative ($P < 0.01$).

CMV DNA was also detected in the preserved umbilical cords from the three positive control patients with congenital CMV infection, but was not detected in the 10 negative controls. Epstein–Barr virus and human herpesvirus 6 DNA were not detected in any of the umbilical cords.

Discussion

Virological diagnosis of congenital CMV infection is not difficult when an infant has characteristic symptoms at birth, such as petechiae, hepatosplenomegaly, jaundice, and microcephaly with calcification. Virological confirmation is made by isolating CMV from urine or detecting CMV DNA in urine or blood of infants within 2 weeks after birth. However, only 10% of congenitally infected babies have signs of infection at birth [17], and most asymptomatic infants are missed during the neonatal period. Retrospective diagnosis of CMV infection in children and adults has been difficult because CMV is ubiquitous. However, several studies have been performed on the retrospective diagnosis of congenital CMV infection by the detection of CMV DNA in umbilical cords or blood stored on Guthrie cards [7, 8, 18, 19]. Blood spots on Guthrie cards are useful to screen for genetic defects or congenital infection, but the cards are not kept long enough or are not always available for retrospective diagnosis of congenital CMV infection. In Japan, the dried umbilical cords of children are traditionally stored in the home as a symbol of the connection between mother and child. In this study, we demonstrated that the DNA in the preserved cord was analyzable for up to 52 years. The detection of CMV DNA from the umbilical cord means that the cells derived from the fetus were infected with CMV. Therefore, the detection directly indicates congenital CMV infection. However, the possibility of contamination from the birth canal does exist, as CMV is detected from genital tract secretions of pregnant women as well as HHV-6. In this study, we concurrently examined whether HHV-6 DNA could be detected from the cords. HHV-6 DNA was not detected in any of the 45 cords, which suggests that contamination was negligible. Our results imply that detecting CMV DNA from preserved

Table 1 Clinical characteristics of each group with SNHL

Groups	No.	Sex		Mean age (years)	No. of affected ears		Mean hearing levels (dB)	
		Male	Female		Right	Left	Affected ears	Difference between right and left ears
A: Sudden SNHL	9	3	6	28.1	4	5	74	65.2
B: EVAs	6	2	4	18.2	6	6	92	11.7
C: Unilateral SNHL	15	9	6	8.6	10	5	88	73.4
D: Bilateral SNHL	15	6	9	10.0	15	15	66	17.8

SNHL sensorineural hearing loss, *EVAs* enlarged vestibular aqueducts

Table 2 Clinical and virologic characteristics of CMV-positive patients with bilateral sensorineural hearing loss

Age (years)	Sex	Hearing level (dB)			Clinical findings	Radiological findings of the inner ear	CMV copy numbers (copies/10^6 cells)
		Right ear	Left ear	Difference			
5	Male	58	115	57	Developmental Delay in Infancy	Normal (CT)	9.6×10^5
6	Female	47	35	12	Mental Retardation	Normal (MRI)	2.8×10^5
9	Female	27	95	68	Hypotonic Muscles	Normal (MRI)	2×10^5

CMV cytomegalovirus, *CT* computed tomography, *MRI* magnetic resonance imaging

umbilical cords is useful for the retrospective diagnosis of congenital CMV infection. We detected CMV DNA in the preserved umbilical cords of three asymmetric SNHL patients. These three patients were missed during the neonatal periods. None of them had typical symptoms for congenital CMV infection at that time. Their developmental delay or hypotonic muscles, and SNHL appeared gradually later. Note that the difference in the hearing level between the right and left ears was larger in patients who were CMV-positive. Asymmetric SNHL is one of the features of congenital CMV infection [4].

Histopathological studies of temporal bones from patients with idiopathic sudden SNHL have suggested viral infection, a vascular origin, or the activation of cellular stress pathways [20–22]. We speculated that cases might exist in which fragility of the inner ear induced by congenital CMV infection was associated with idiopathic sudden SNHL. However, CMV DNA was not detected in any of the patients with idiopathic sudden SNHL or EVA-associated SNHL. These results suggest that a relationship between congenital CMV infection and sudden SNHL and EVA-associated SNHL does not exist.

Ganciclovir is widely used for the treatment of immunosuppressed patients with symptomatic CMV infection, particularly solid organ and bone marrow transplant recipients and AIDS patients. Ganciclovir is also used for the treatment of symptomatic congenital CMV infection. To improve the prognosis of congenital CMV infection, the efficacy of ganciclovir treatment has been evaluated, and a recent phase II clinical study demonstrated that ganciclovir treatment could reduce or stabilize hearing impairment [23, 24]. Other studies have also suggested that ganciclovir is potentially effective for CMV-associated SNHL [25, 26]. We previously reported that CMV DNA was detected in perilymph specimens obtained from two patients who had been diagnosed with congenitally symptomatic CMV infection [27]. The two patients were 2 and 3 years old at the time of the investigation. This result indicates that CMV replicates in the inner ear for several years in patients with symptomatic congenital CMV infection. These facts suggest that late ganciclovir therapy could be effective for patients with SNHL associated with congenital CMV infection. Therefore, retrospective diagnosis of congenital CMV infection is particularly important for SNHL having an unknown etiology.

Conclusion

Using real-time PCR, CMV DNA was detected in the umbilical cords of three patients with bilateral SNHL without a clear onset period. This method is useful for the retrospective diagnosis of congenital CMV infection. Moreover, a relationship between congenital CMV infection and sudden SNHL or EVA-associated SNHL does not appear to exist. The hearing loss of CMV-associated SNHL was more asymmetric than CMV-negative bilateral SNHL.

Acknowledgments This study was supported by the Acute Profound Deafness Committee of the Ministry of Health, Labour and Welfare, Japan.

References

1. Demmler GJ (1991) Infectious disease society of america and centers for disease control. Summary of a workshop on surveillance for congenital cytomegalovirus disease. Rev Infect Dis 13:315–329
2. Fowler KB, McCollister FP, Dahle AJ, Boppana S, Britt WJ, Pass RF (1997) Progressive and fluctuating sensorineural hearing loss in children with asymptomatic congenital cytomegalovirus infection. J Pediatr 130:624–630
3. Fowler KB, Stagno S, Pass RF, Britt WJ, Boll TJ, Alford CA (1992) The outcome of congenital cytomegalovirus infection in relation to maternal antibody status. N Eng J Med 326:663–667
4. Dahle AJ, Fowler KB, Wright JD, Boppana SB, Britt WJ, Pass RF (2000) Longitudinal investigation of hearing disorders in children with congenital cytomegalovirus. J Am Acad Audiol 11:283–290
5. Jackler RK, De La Cruz A (1989) The large vestibular aqueduct syndrome. Laryngoscope 99:1238–1242
6. Griffith AJ, Arts A, Downs C, Innis JW, Shepard NT, Sheldon S, Gebarski SS (1996) Familial large vestibular aqueduct syndrome. Laryngoscope 106:960–965
7. Koyano S, Araki A, Hirano Y, Fujieda K, Suzutani T, Yagyu K, Murono K, Inoue N (2004) Retrospective diagnosis of congenital cytomegalovirus infection using dried umbilical cords. Pediatr Infect Dis J 5:481–482
8. Kakizawa H, Okumura A, Suzuki Y, Natsume J, Kimura H, Negoro T, Watanabe K (2005) Congenital cytomegalovirus infection diagnosed by polymerase chain reaction with the use of preserved umbilical cord. Pediatr Infect Dis J 24:653–654
9. Ogawa H, Baba Y, Suzutani T, Inoue N, Fukushima E, Omori K (2006) Congenital cytomegalovirus infection diagnosed by polymerase chain reaction with the use of preserved umbilical cord in sensorineural hearing loss children. Laryngoscope 116:1991–1994
10. Ikeda S, Tsuru A, Moriuchi M, Moriuchi H (2006) Retrospective diagnosis of congenital cytomegalovirus infection using umbilical cord. Pediatr Neurol 34:415–416
11. Ogawa H, Suzutani T, Baba Y, Koyano S, Nozawa N, Ishibashi K, Fujieda K, Inoue N, Omori K (2007) Etiology of severe sensorineural hearing loss in children: independent impact of congenital cytomegalovirus infection and GJB2 mutations. J Infect Dis 195:782–788
12. Yasuda A, Kimura H, Hayakawa M, Ohshiro M, Kato Y, Matsuura O, Suzuki C, Morishima T (2003) Evaluation of cytomegalovirus infections transmitted via breast milk in preterm infants with a real-time polymerase chain reaction assay. Pediatrics 116:1333–1336
13. Tanaka N, Kimura H, Iida K, Saito Y, Tsuge I, Yoshimi A, Matsuyama T, Morishima T (2000) Quantitative analysis of cytomegalovirus load using a real-time PCR assay. J Med Virol 60:455–462
14. Akrigg A, Wilkinson GW, Oram JD (1985) The structure of the major immediate early gene of human cytomegalovirus strain AD169. Virus Res 2:107–121
15. Kimura H, Morita M, Yabuta Y, Kuzushima K, Kato K, Kojima S, Matsuyama T, Morishima T (1999) Quantitative analysis of

Epstein–Barr virus load by using a real-time PCR assay. J Clin Microbiol 37:132–136
16. Tanaka N, Kimura H, Hoshino Y, Kato K, Yoshikawa T, Asano Y, Horibe K, Kojima S, Morishima T (2000) Monitoring four herpesviruses in unrelated cord blood transplantation. Bone Marrow Transplant 26:1193–1197
17. Pass RF, Stagno S, Myers GJ, Alford CA (1980) Outcome of symptomatic congenital cytomegalovirus infection: results of long-term longitudinal follow-up. Pediatrics 66:758–762
18. Haginoya K, Ohura T, Kon K, Yagi T, Sawaishi Y, Ishii K, Funato T, Higano S, Takahashi S, Iinuma K (2002) Abnormal white matter lesions with sensorineural hearing loss caused by congenital cytomegalovirus infection: retrospective diagnosis by PCR using Guthrie cards. Brain Dev 24:710–714
19. Johansson PJ, Jonsson M, Ahlfors K, Ivarsson IA, Lars S, Guthenberg C (1997) Retrospective diagnostics congenital cytomegalovirus infection performed by polymerase chain reaction in blood stored on filter paper. Scand J Infect Dis 29:465–468
20. Schuknecht HF, Kimura RS, Naufal PM (1973) The pathology of sudden deafness. Acta Otolaryngol 76:76–97
21. Vasama JP, Linthicum JR (2000) Idiopathic sudden sensorineural hearing loss: temporal bone histopathologic study. Ann Otol Rhinol Laryngol 109:527–532
22. Merchant SN, Adams JC, Nadol JB Jr (2005) Pathology and pathophysiology of idiopathic sudden sensori neural hearing loss. Otol Neurotol 26:151–160
23. Whitley RJ, Cloud G, Gruber W, Storch GA, Demmler GJ, Jacobs RF, Dankner W, Spector SA, Starr S, Pass RF, Stagno S, Britt WJ, Alford C Jr, Soong S, Zhou XJ, Sherrill L, FitzGerald JM, Sommadossi JP (1997) The National Institute of allergy, Infectious Diseases Collaborative Antiviral Study Group Ganciclovir treatment of symptomatic congenital cytomegalovirus infection: result of a phase II study. J Infect Dis 175:1080–1086
24. Kimberlin DW, Lin CY, Sanchez PJ, Demmler GJ, Dankner W, Shelton M, Jacobs RF, Vaudry W, Pass RF, Kiell JM, Soong S, Whitley RJ (2003) Effect of ganciclovir therapy on hearing in symptomatic congenital cytomegalovirus disease involving the central nervous system: a randomized, controlled trial. J Pediatr 143:16–25
25. Tanaka-Kitajima N, Sugaya N, Futatani T, Kanegane H, Suzuki C, Oshiro M, Hayakawa M, Futamura M, Morishima T, Kimura H (2005) Ganciclovir therapy for congenital cytomegalovirus infection in six infants. Pediatr Infect Dis J 24:782–785
26. Michaels MG, Greenberg DP, Sabo DL, Wald ER (2003) Treatment of children with congenital cytomegalovirus infection with ganciclovir. Pediatr Infect Dis J 22:504–509
27. Sugiura S, Yoshikawa T, Nishiyama Y, Morishita Y, Sato E, Beppu R, Hattori T, Nakashima T (2004) Detection of herpesvirus DNAs in perilymph obtained from patients with sensorineural hearing loss by real-time polymerase chain reaction. Laryngoscope 114:2235–2238

Acta Oto-Laryngologica, 2009; Early Online, 000–000

informa
healthcare

ORIGINAL ARTICLE

3D-FLAIR MRI in facial nerve paralysis with and without audio-vestibular disorder

SEIICHI NAKATA[1], TERUKAZU MIZUNO[1,3], SHINJI NAGANAWA[2], MAKOTO SUGIURA[1,4], TADAO YOSHIDA[1], MASAAKI TERANISHI[1], MICHIHIKO SONE[1] & TSUTOMU NAKASHIMA[1]

[1]*Department of Otorhinolaryngology and* [2]*Department of Radiology, Nagoya University Graduate School of Medicine, Nagoya,* [3]*Department of Otorhinolaryngology, Komaki Municipal Hospital, Komaki and* [4]*Department of Otorhinolaryngology, Kariya Toyota General Hospital, Kariya, Japan*

Abstract

Conclusion: Among patients with facial nerve paralysis, significant difference was observed on three-dimensional fluid-attenuated inversion recovery magnetic resonance imaging (3D-FLAIR MRI) between those with and without audio-vestibular disturbance. This MRI technique may contribute to elucidation of the pathology of Ramsay Hunt syndrome and Bell's palsy. *Objective:* To evaluate the 3D-FLAIR MRI findings in patients who have facial nerve paralysis with and without audio-vestibular disturbance. *Methods:* 3D-FLAIR MRI was performed with and without gadolinium enhancement in 15 patients (5 men and 10 women) with unilateral facial nerve paralysis: 3 patients with Ramsay Hunt syndrome, 3 patients having facial nerve paralysis with hearing loss or vertigo without vesicles, and 9 patients with Bell's palsy. *Results:* Five of the six patients with audio-vestibular disturbance showed high signals in the inner ear on precontrast 3D-FLAIR. In comparison, among nine patients with Bell's palsy, only one patient showed high signals in the inner ear on precontrast 3D-FLAIR ($p < 0.05$).

Keywords: *Bell's palsy, Ramsay Hunt syndrome, inner ear*

Introduction

Facial nerve paralysis can be caused by a variety of unknown pathophysiological mechanisms, although many cases have been associated with a varicella-zoster virus (VZV) or herpes simplex virus infection. In some cases, it is very difficult to distinguish Ramsay Hunt syndrome from Bell's palsy, even by immunological examinations or imaging studies, such as magnetic resonance imaging (MRI) [1].

Three-dimensional fluid-attenuated inversion recovery (3D-FLAIR) MRI has been developed to detect haemorrhage or high concentrations of proteins, which are difficult to detect by T1- or T2-weighted MRI. Subtle high-signal areas in the cerebrospinal fluid (CSF) can be an indicator of subarachnoid haemorrhage, meningitis, or acute infarction. We have reported previously that CSF-related flow artefacts are significantly lower on 3D-FLAIR images than on 2D-FLAIR images [2]. Using 3D-FLAIR MRI at 3 Tesla (T), high signals in the inner ear have been shown in patients with various inner ear diseases, such as idiopathic sudden sensorineural hearing loss [3,4], cochlear otosclerosis [5], mumps deafness [6] and cholesteatoma with labyrinthine fistula [7]. These signals may reflect minor haemorrhage or an increased concentration of protein in the inner ear, which has passed through blood vessels with increased permeability.

Findings of high signal in the affected ear of a patient with Ramsay Hunt syndrome examined with 3D-FLAIR were reported for the first time by

Correspondence: Seiichi Nakata MD, Department of Otorhinolaryngology, Nagoya University Graduate School of Medicine 65, Tsurumai-cho, Showa-ku, Nagoya 466-8550, Japan. Tel: +81 52 744 2323. Fax: +81 52 744 2325. E-mail: seisay@med.nagoya-u.ac.jp

(Received 09 May 2009; accepted 08 July 2009)

ISSN 0001-6489 print/ISSN 1651-2251 online
DOI: 10.3109/00016480903338123

Sugiura et al. [8]. However, the differences in the 3D-FLAIR MRI findings between Ramsay Hunt syndrome and Bell's palsy have not been clarified. Accordingly, we investigated the 3D-FLAIR MRI findings in facial nerve paralysis patients with audio-vestibular disorder, who were classified as having Ramsay Hunt syndrome and atypical Bell's palsy, and in those without audio-vestibular disorder who were classified as having Bell's palsy in the present study.

Material and methods

Subjects

We evaluated 15 patients (5 men and 10 women; mean age ± SD, 47.3 ± 16.6 years) with unilateral facial nerve paralysis, who visited our hospital between February 2006 and February 2008. We diagnosed the patients as having Ramsay Hunt syndrome when they had symptoms of eighth nerve dysfunction (tinnitus, hearing loss and vertigo) and a vesicle on an external auditory meatus or auricle including symptoms of seventh nerve dysfunction. We diagnosed the patients as having Bell's palsy when they initially had only symptoms of seventh nerve dysfunction with no vesicle on an external auditory meatus or auricle [9]. Moreover, we diagnosed the patients as having atypical Bell's palsy when they had symptoms of eighth nerve dysfunction (tinnitus, hearing loss and vertigo) with no vesicle on an external auditory meatus or auricle including symptoms of seventh nerve dysfunction.

The mean ages of the three patients with Ramsay Hunt syndrome (three women), the three atypical Bell's palsy patients (two men and a woman) and the nine patients with Bell's palsy (three men and six women) were 50.3 ± 20.7, 40.7 ± 13.6 and 46.2 ± 17.7 years, respectively. Then, we reclassified these patients into two categories of facial nerve paralysis, those with and those without audio-vestibular disorder. Both Ramsay Hunt syndrome and atypical Bell's palsy were classified as facial nerve paralysis with audio-vestibular disorder, while Bell's palsy patients were classified as having facial nerve paralysis without audio-vestibular disorder. The initial House-Brackmann scale [10] score of the patients with facial nerve paralysis was IV in 4 cases, V in 10 cases, and VI in 1 case (Table I). In all patients, hydrocortisone was administered intravenously at 200 mg per day for 4 consecutive days, and then at 100 mg per day for 3 consecutive days, with adenosine triphosphate (80 mg per day). All the patients were treated with valacyclovir (3000 mg per day for 7 days) to preclude infection by VZV.

MRI

All MRI scans were performed using a 3 T magnet (Trio, Siemens, Erlangen, Germany) and a receive-only

Table I. Characteristics of patients with facial nerve paralysis.

Patient no.	Age (years)	Gender	Diagnosis	Grade of palsy (onset)	Serological VZV reactivation
1	28	F	Ramsay Hunt syndrome	IV	–
2	54	F	Ramsay Hunt syndrome	VI	–
3	69	F	Ramsay Hunt syndrome	V	+
4	56	F	Atypical Bell's palsy	V	+
5	36	M	Atypical Bell's palsy	V	+
6	30	M	Atypical Bell's palsy	IV	–
7	58	F	Bell's palsy	V	–
8	38	F	Bell's palsy	V	–
9	49	M	Bell's palsy	V	–
10	27	F	Bell's palsy	IV	–
11	78	M	Bell's palsy	V	–
12	24	F	Bell's palsy	V	–
13	31	F	Bell's palsy	IV	–
14	57	F	Bell's palsy	V	–
15	54	M	Bell's palsy	V	–

Patient nos 1, 7, 9, 11 and 14 underwent serology only at their initial visit (IgM negative).